Strong nonlocal contributions to Cu 2*p* photoelectron spectroscopy

M. A. van Veenendaal, H. Eskes, and G. A. Sawatzky
Laboratory of Applied and Solid State Physics, Materials Science Centre, University of Groningen, Nijenborgh 4, 9747 AG Groningen, The Netherlands
(Received 25 November 1992)

Calculations of Cu 2*p* photoelectron spectra for a Cu_3O_{10} cluster with a reduced basis set show that the introduction of more Cu sites leads to a revised interpretation of the Cu 2*p* spectrum. Besides the usual peaks of mainly $3d^9$ and $3d^{10}\underline{L}$ character another peak appears at lower binding energy. This peak is of mainly $3d^{10}$ character. The hole has moved away from the core hole potential and has formed a Zhang-Rice singlet on a neighboring CuO_4 unit. This effect explains the asymmetric line shape of the main line in the Cu 2*p* spectra of CuO and the high-T_c compounds. For formally trivalent copper compounds, such as $NaCuO_2$, this effect disappears and a narrow line shape is observed. The consequences of hole doping (33%) on the Cu 2*p* spectra have also been studied. The peak assignment turns out to be very similar to that of the undoped system.

I. INTRODUCTION

The structure of the core levels in x-ray photoelectron spectroscopy has been and continues to be a field of extensive research. For transition-metal and rare-earth compounds the core levels often show pronounced satellite structures. In the last $2\frac{1}{2}$ decades a large number of explanations have been proposed to elucidate the underlying physics of these structures. At first they were interpreted as shake up structures, e.g., $3d-4s4p$ (Ref. 1) or ligand to metal excitations (Ref. 2). This implies that the electronic configuration of the valence electrons for the lowest final state is equivalent to that of the ground state. Subsequent theories incorporated the effect of screening of the core hole potentials by electrons coming from the surrounding ligands.[3–5] The satellite structure is now a result of the non-negligible overlap of the ground state and the unscreened final state.

In recent years this explanation has become more generally accepted. The use of model Hamiltonians, e.g., Anderson impurity[6,7] or cluster calculations,[5,7] made it possible to use core-level photoelectron spectroscopy as a tool to determine properties of transition-metal[8–10] and rare-earth compounds.[11–13] After the discovery of the high-T_c superconductors, the Cu 2*p* core level has provided information on, e.g., the strongly correlated nature of these systems and the valency of the Cu atoms in the planes.[14] It has also been used to estimate a number of important parameters, such as, e.g., the charge-transfer energy.[14–16]

However, a number of features of the Cu 2*p* spectrum are still not well understood. First, the main line has a large width, which cannot be explained in terms of experimental resolution and lifetime broadening. This width is usually interpreted as a consequence of the fact that the main line has mainly $d^{10}\underline{L}$ character and should thus show a substantial width due to the oxygen bandwidth.[6,7] However, following this interpretation it is surprising that $NaCuO_2$ has a narrow main line, where this peak is supposedly of $d^{10}\underline{L}^2$ character. Karlsson, Gunnarsson, and Jepsen[17] interpreted this by taking into account a more realistic oxygen band. The small width of the main line they proposed to be a result of the fact that the matrix elements are strongly peaked toward the top of the oxygen band. Others ascribe the large width to a fluctuating charge state,[18] where the Cu 2*p* spectrum is a superposition of a Cu 2*p* spectrum comparable to that of Cu_2O and a Cu 2*p* spectrum similar to CuO, but with a narrow main line.

Second, there seems to be a systematic discrepancy between parameters obtained from valence band and Cu 2*p* spectra. For Cu 2*p* one usually finds a lower value of the charge-transfer energy.[14–16] Third, the behavior of the Cu 2*p* spectra upon hole doping is not well understood. Usually the difference between the doped and the undoped spectrum is interpreted in a similar way as the Cu 2*p* spectrum of $NaCuO_2$, i.e., the main line is of mainly $d^{10}\underline{L}^2$ character and the satellite of $d^9\underline{L}$ character, see, e.g., DeSantis *et al.*[19] and Steiner *et al.*[20]

Little, however, has been done so far in the study of the effects caused by the presence of other Cu sites on the Cu 2*p* spectrum. This was justified by the assumption that the Cu 2*p* spectrum is mainly determined by local properties. In this paper we will show that increasing the cluster size leads to a revised interpretation of the spectrum.

The organization of this paper is as follows. First, the cluster that we have used, i.e., a Cu_3O_{10} cluster, will be introduced. Then a brief recapitulation of the Cu 2*p* spectrum of a system with one Cu impurity will be given. Subsequently the consequences of introducing other copper sites will be discussed. We will also study the effect of hole doping and compare the calculations with experiment.

II. DESCRIPTION OF THE MODEL

In our model we made use of similar types of clusters used earlier in the work of Eskes and co-workers.[21–23] They studied the effects of doping on photoemission, in-

 ©1993 The American Physical Society

verse photoemission, and various other kinds of high-energy spectroscopy with a Cu_2O_7 cluster. In this study we have looked at CuO_4, Cu_2O_7, and Cu_3O_{10} clusters (see Fig. 1). To limit the size of the problem a reduced basis set has been used. For CuO and the high-T_c compounds the appropriate symmetry is D_{4h}. The large hybridization causes a ligand field splitting. In D_{4h} symmetry the d states will branch into a_1, b_1, b_2, and e irreducible representations. These states will hybridize with linear combinations of oxygen orbitals of the same symmetry. The ligand field splitting is a consequence of two effects: First, the oxygen orbitals in the different symmetries have different energies due to the oxygen-oxygen hybridization and second, the p-d hybridization elements vary for the different symmetries, thereby also taking into account that the σ bonding matrix element is about twice as large as the π bonding. The ligands have the largest effect on the energy of the b_1 symmetry, which corresponds to the x^2-y^2 orbital. As a reduced basis set we have therefore used the Cu $3d_{x^2-y^2}$ orbital and the σ bonding O $2p$ orbitals.

For the calculation of, e.g., Cu $2p$, inverse photoemission spectroscopy and O $1s$ x-ray-absorption spectroscopy,[24] this is an adequate basis set. This is in contrast with, e.g., x-ray photoemission spectroscopy, where the overall shape of the valence band is mainly determined by emission from the other Cu $3d$ orbitals.[21–23] In core-level spectroscopy, however, the number of valence electrons does not change so that a reduced basis set involving only $d_{x^2-y^2}$ orbitals is probably appropriate. A comparison of Cu $2p$ spectra for a Cu_2O_7 cluster calculated with a full basis set and with a reduced basis set support the use of this approximation (see Fig. 2) (for the interpretation, see below). For two holes, i.e., one per Cu site, the agreement is excellent. For three holes (50% hole doping) there are only small differences in the shape of the satellite. These are most likely caused by the neglect of the Cu $3d^8$ Coulomb interaction between Slater determinants with the same symmetry as $|d_{x^2-y^2\uparrow}d_{x^2-y^2\downarrow}\rangle$ and by the presence of hole density in the Cu $3d_{3z^2-r^2}$ orbitals for the full basis set.

The Hamiltonian (in hole notation) for the reduced basis set consists of three parts,

$$H=H_0+H_1+H_c \ .$$

The one particle part H_0 is given by

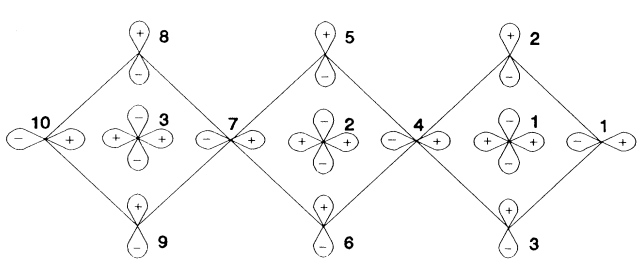

FIG. 1. The Cu_3O_{10} cluster used in the calculations. The $3d_{x^2-y^2}$ are numbered up to three. The σ bonding O $2p$ orbitals are numbered from 1 to 10.

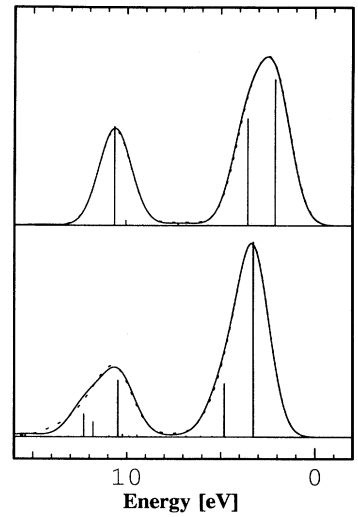

FIG. 2. Comparison of the Cu $2p$ spectra calculated with a full basis set (dashed line) and a reduced basis set (solid line). The poles correspond to the reduced basis set. The upper half is the calculation for two holes, the lower for three holes (50% doping).

$$H_0=\sum_{i,\sigma}\varepsilon_{x^2-y^2}d^\dagger_{i,\sigma}d_{i,\sigma}+\sum_{j,\sigma}\varepsilon_p p^\dagger_{j,\sigma}p_{j,\sigma}$$
$$+\sum_{i,j,\sigma}[t_{pd}(i,j)d^\dagger_{i,\sigma}p_{j,\sigma}+\text{H.c.}]$$
$$+\sum_{j,j',\sigma}[t_{pp}(j,j')p^\dagger_{j,\sigma}p_{j',\sigma}+\text{H.c.}] \ ,$$

where the summations i and j go over the different Cu $3d_{x^2-y^2}$ and σ bonding O $2p$ orbitals, respectively (see Fig. 1). The first two summations count the holes in the different orbitals. The index x^2-y^2 in the hole annihilation operator $d_{i,\sigma}$ and its conjugate has been dropped for clarity. The next term describes the hybridization between the $d_{x^2-y^2}$ and the nearest-neighbor O $2p$ orbital, where $|t_{pd}(i,j)|=\frac{1}{2}\sqrt{3}(pd\sigma)$ in terms of Slater Koster integrals.[26] The last term describes the hopping between two nearest-neighbor oxygen orbitals. The size of the matrix element $|t_{pp}(j,j')|$ is $\frac{1}{2}[(pp\pi)-(pp\sigma)]$.

The interaction between holes on copper and on oxygen is described by H_1,

$$H_1=\sum_i U_d n_{i,\uparrow}n_{i,\downarrow}+\sum_j U_p n_{j,\uparrow}n_{j,\downarrow} \ ,$$

with $U_d=A+4B+3C$ in terms of Racah parameters.

The last part of the Hamiltonian, H_c, describes the interaction between the Cu $2p$ core hole and a hole in the Cu $3d_{x^2-y^2}$ orbital on the same site,

$$H_c=\sum_{i,\sigma}Qd^\dagger_{i,\sigma}d_{i,\sigma}c^\dagger_i c_i+\sum_i E_{2p}c^\dagger_i c_i \ ,$$

where $c^\dagger_i$ annihilates a core electron at site i. E_{2p} is the energy of the Cu $2p$ core hole. In the interaction Q all multiplet effects between the core hole and the $3d$ hole have been neglected. Although the multiplet structure is important in understanding the shape of the satellite it

hardly affects the intensity ratio or the energy difference between the satellite and the main peak.[27]

In the calculation we make use of the relation between the spectral distribution $I(E_k)$ and the one-hole Green's function $g_i^c(z)$,

$$I(E_k) \sim \frac{1}{\pi} \mathrm{Im}[g_i^c(\hbar\omega + E_0 - E_k - i0^+)] ,$$

where $\hbar\omega$ is the energy of the incoming photon and E_k the kinetic energy of the outgoing photoelectron. The Green's function is defined as

$$g_i^c(z) = \langle E_0 | c_i \frac{1}{z-H} c_i^\dagger | E_0 \rangle ,$$

where $|E_0\rangle$ is the ground-state wave function. In most of the calculations the core hole is removed from the central Cu site. The Green's function is evaluated using a continued fraction expansion.

III. THE Cu 2p SPECTRUM WITH A SINGLE Cu ATOM

Before discussing the effects of the other Cu atoms, we will first briefly recapitulate the situation with one Cu atom. For this case the nature of the satellite and the main peak can be most simply understood by considering a single Cu site surrounded by four oxygens in a square planar symmetry. In an ionic picture copper would be $3d^9$ and the oxygen orbitals would be completely filled.

The one-hole ground state can be written as a linear combination of a state with a hole in a $|d_{x^2-y^2}\rangle$ orbital and a state with the hole in a linear combination of oxygen $2p$ orbitals with the same symmetry,

$$|p_{x^2-y^2}\rangle = \tfrac{1}{2}\{|p_{x1}\rangle - |p_{x4}\rangle - |p_{y2}\rangle + |p_{y3}\rangle\}$$

(for the convention of the orbitals see Fig. 1),

$$|1 \text{ hole}\rangle = \sqrt{n_d}|d_{x^2-y^2}\rangle + \sqrt{1-n_d}|p_{x^2-y^2}\rangle ,$$

where n_d is the Cu $3d$ hole count. The final state basis set is equivalent, except for the presence of the core hole: $|\underline{c}d_{x^2-y^2}\rangle$ and $|\underline{c}p_{x^2-y^2}\rangle$. The Hamiltonian for the ground as well as the final state can now be written, in matrix form, as

$$H = \begin{bmatrix} Q\langle n_c \rangle & 2t_{pd} \\ 2t_{pd} & \Delta - 2t_{pp} \end{bmatrix} ,$$

where Δ is the energy difference between a hole in an O $2p$ orbital and hole in a Cu $3d$ orbital, $\varepsilon_p - \varepsilon_d$. For a linear combination of O $2p$ orbitals in b_1 symmetry this energy is lowered by $2t_{pp}$, as a result of the direct hopping between the oxygen orbitals. The diagonal element for $|d_{x^2-y^2}\rangle$ contains the Coulomb repulsion between the Cu $2p$ core hole and the $3d$ hole, $Q\langle n_c \rangle$. For the ground state, where there is no core hole, i.e., $\langle n_c \rangle = 0$, this term vanishes. The hybridization between the two hole states of b_1 symmetry is $2t_{pd}$. Using the parameter set of Table I, the ground state can now be written as

$$|1 \text{ hole}\rangle = \sqrt{0.69}|d_{x^2-y^2}\rangle + \sqrt{0.31}|p_{x^2-y^2}\rangle .$$

TABLE I. Parameters values used for all the different clusters. All energies in eV.

$\varepsilon_p - \varepsilon_d$	3.5
$pd\sigma$	1.5
$pp\sigma$	−1.0
$pp\pi$	0.3
U_d	8.8
U_p	6.0

This leads to 9.31 electrons on the Cu site, which is considerably more than for a simple ionic compound.

The Cu $2p$ spectrum now consists of two peaks, whose intensity is determined by the overlap of the ground state and the two final states. The result is given in Fig. 3(a). The lowest eigenstate has now mainly $d^{10}\underline{L}$ character, the Cu $3d$ hole count has dropped here to 0.1. The extra $3d$ electron provides a better screening of the core hole potential. The satellite region has mainly $3d^9$ character and appears at higher binding energies due to the repulsion of the $3d$ hole by the core hole. This explanation also corresponds very well with the observation by Van der Laan *et al.*,[5] that for copper halides the shape of the satellite resembles the $2p^5 3d^9$ atomic multiplet structure.

For this calculation a well-established parameter set has been used. The values have been obtained by a careful comparison of calculated valence-band spectra with those obtained by high-energy spectroscopy[22,23] (through out the paper, except for the value of Q, the same parameter set will be used, see Table I). These values agree very well with those obtained by contrained local-density approximation calculations.[28,29]

The energy difference between the main peak and the satellite peak is given by $[(Q-\Delta+2t_{pp})^2+16t_{pd}^2]^{1/2}$. In order to reproduce the right splitting between the main peak and the satellite, which we will take to be some-

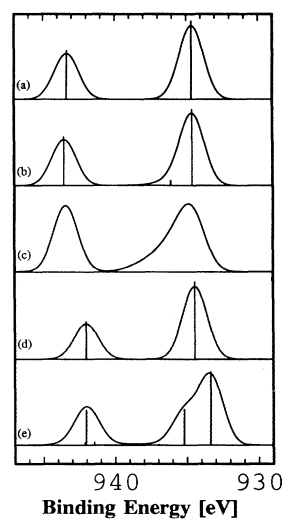

FIG. 3. Cu $2p$ spectra for undoped systems using different clusters. From top to bottom: (a) CuO_4 cluster with one hole, $Q=9.2$; (b) CuO_{10} cluster with one hole, $Q=9.2$; (c) Anderson impurity calculation, $Q=9.2$; (d) CuO_4 cluster with one hole, $Q=7.7$; (e) Cu_3O_{10} cluster with three holes, $Q=7.7$.

where around 8.7 eV, a value of Q of 9.2 eV is needed. However, when comparing this result with experimental data, one sees a number of discrepancies. First of all, the calculation gives an anomalously high value of 0.62 of the intensity ratio of the satellite and the main peak. This should be compared with an experimental value of 0.3–0.4. To correct for this difference one has two options: either raising the hybridization or a decrease of the charge-transfer energy. Since the former is well established by band-structure calculations, the latter possibility is usually chosen. This has resulted in very small values of the charge-transfer energy[14,15] or, in the case of Anderson impurity models, estimations where the Cu 3d level is in the oxygen band.[16]

Second, it does not reproduce the width and asymmetry of the main peak. This might be a result of the neglect of the oxygen bandwidth. To study the effects of other oxygen atoms two different systems have been studied. First, we have looked at a CuO_{10} cluster. This is equivalent to the Cu_3O_{10} cluster, introduced in the preceding paragraph, but with the Cu atoms on the left and on the right side of the cluster removed. The Cu 2p spectrum for this cluster with one hole is shown in Fig. 3(b). The spectrum is very similar to the one obtained by the CuO_4 cluster. It is straightforward to show that of the ten different oxygen orbitals only four linear combinations mix with the $d_{x^2-y^2}$ orbital due to symmetry reasons. These four states also appear in the Cu 2p spectrum and are spread over an energy range of the order of the oxygen bandwidth, i.e., over more than 4 eV, but only one pole has significant weight. The reason is that for the lowest eigenstate in both ground and final state the hole is mainly localized on the Cu site plus its four surrounding oxygens. Band effects are therefore expected to be small.

Similar effects are also observed in Anderson impurity calculations [see Fig. 3(c)]. For this calculation the basis set consisted of a $d_{x^2-y^2}$ orbital and a semielliptical oxygen band with a bandwidth of $8t_{pp}$ (for more details see, e.g., Refs. 6 and 7). The main peak is of $3d^{10}\underline{L}$ character, therefore its width is proportional to the oxygen bandwidth. However the intensity is skewed towards the top of the oxygen band. Furthermore, in an Anderson impurity framework it is not very straightforward to explain the narrow main line of $NaCuO_2$ unless when this is an effect of a peculiar shape of the hybridization matrix elements, as was proposed by Karlsson, Gunnarsson, and Jepsen.[17] Another point is that the Anderson impurity also has a high satellite to main intensity ratio, when valence-band parameters are used.

In the rest of this paper we will show that the large width of the main line and the discrepancies between parameters needed to describe Cu 2p and valence-band spectra are due to an inadequacy in the treatment of Cu 2p spectra. So far it has been assumed that the spectra were mainly determined by local properties. Therefore the calculations have been mainly restricted to one single Cu atom. However the strong repulsion between the core hole and the 3d hole necessitates the presence of other copper sites in the calculation, as will be discussed in the following paragraph.

IV. Cu 2p SPECTRA WITH MORE Cu ATOMS

The Cu 2p spectrum for a Cu_3O_{10} cluster with three holes is shown in Fig. 3(e) [see also 6(b)]. The value of Q needed to reproduce the energy splitting between the main line and the satellite is 7.7 eV. (The value of E_p has been adjusted in such a way that the top of the main peak coincides with that of the experimental data to be discussed below.) For comparison, Fig. 3(d) shows the Cu 2p spectrum calculated with a CuO_4 cluster for the same value of Q. Note that the splitting between the main and the satellite peak is much smaller for the CuO_4 cluster compared to the Cu_3O_{10} cluster. The major effect for the Cu_3O_{10} cluster is that the main line now consists of two poles, which results in a much broader main line. For this calculation also, a much better satellite to main intensity ratio of 0.4 is found.

To examine the nature of these poles we have looked at the hole densities on various sites (see Fig. 4). For the ground state the hole distribution is shown in Fig. 4(a). This can be most easily understood as three separate CuO_4 clusters, see, also, the Introduction. Thereby taking into account that the connecting oxygen orbitals 4

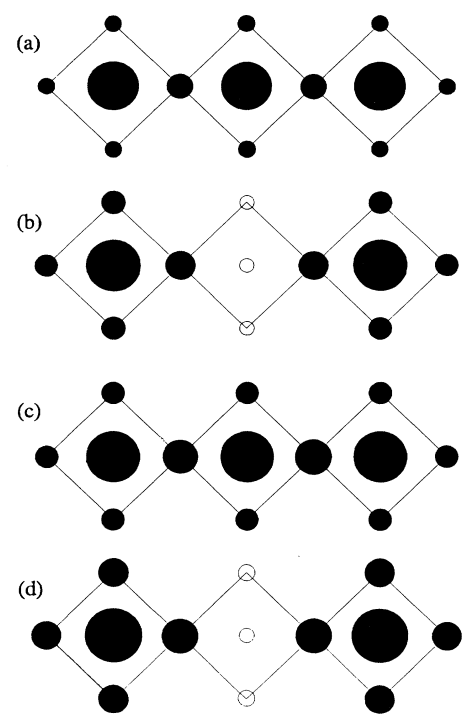

FIG. 4. Hole densities for the Cu_3O_{10} cluster. The area of the circles corresponds to the hole density. From top to bottom: (a) three hole ground-state distribution, (b) three holes with a Cu 2p hole on the central Cu site [the open circles indicate a decrease in hole density with respect to (a)], (c) for hole ground-state distribution, (d) four holes with a Cu 2p hole on the central Cu site [the open circles indicate a decrease in hole density with respect to (c)]. The hole densities in (b) and (d) correspond to the lowest final states of the Cu 2p spectra in Figs. 3(e) and 6(d), respectively.

and 7 (see Fig. 1) are shared by two $|p_{x^2-y^2}\rangle$ states and therefore have twice as much hole density as the other oxygens. The hole density in copper is about 4% lower than in the CuO_4 cluster. Note also that the finite-size effects are rather small. The hole density on the CuO_4 units on the left and on the right side of the cluster is only slightly smaller compared to the one in the center (thereby equally dividing the hole densities on the connecting oxygen over the two neighboring CuO_4 units). The major difference is that the hole density on the connecting oxygens is relatively large compared to the orbitals at the edges of the cluster.

The same procedure has been applied to the lowest eigenstate of the final state, i.e., the peak with the lowest binding energy in the Cu 2*p* spectrum of Fig. 3(e). This is shown in Fig. 4(b). For a CuO_4 cluster the effect of making a core hole is that the Coulomb repulsion causes the lowest final state to be of mainly $|p_{x^2-y^2}\rangle$ character. One therefore expects a large increase of the hole density on the oxygens surrounding the central copper site. However one sees immediately that there is a decrease of hole density on oxygen orbitals 5 and 6, combined with an increase in hole density on all the orbitals of the CuO_4 units at the edges of the cluster. If we again calculate the hole density on the central CuO_4 unit, in a similar way as was done above, we see that this has dropped to 0.4 hole. *This implies that the lowest eigenstate of a Cu 2p spectrum is not of mainly $3d^{10}\underline{L}$ character but of mainly d^{10} character, with the hole now on a neighboring CuO_4 unit.*

It can be most easily seen that this is energetically more favorable by considering two separate CuO_4 clusters (see the energy diagram of Fig. 5). In the ground state it is obvious that placing one hole on each CuO_4 cluster is energetically the most favorable solution [see Fig. 5(b)]. However after removal of the Cu 2*p* core electron the situation is less clear, whether it is more advantageous to put one hole on each CuO_4 cluster or to put both holes on the cluster without the core hole [see Figs. 5(c) and 5(d)]. For $t_{pd}=0$, the lowest energy is $\Delta-2t_{pp}$ in both cases. This means that one of the holes is on the oxygens. In the first case this is a result of the strong core hole potential, in the second this is due to the Coulomb interaction when both holes would be on the Cu site. However after switching on the hybridization the energy for the situation with two holes on the cluster without the core hole is about 0.64 eV lower than the situation with one hole on each cluster. This should be attributed to the fact that the stabilization energy of two holes on one CuO_4 cluster is relatively large. These two holes form a so-called Zhang-Rice singlet.[30] This state, which has a ${}^1A_1$ symmetry[25] has a wave function,

$$|2\text{ holes ZR}\rangle=\sqrt{0.68}|d_{x^2-y^2}p_{x^2-y^2}\rangle+\sqrt{0.23}|p^2_{x^2-y^2}\rangle+\sqrt{0.09}|d^2_{x^2-y^2}\rangle\ ,$$

with mainly $|d_{x^2-y^2}p_{x^2-y^2}\rangle$ character. As can be seen from Figs. 5(c) and 5(d), the energy difference with the next configuration is $\Delta-2t_{pp}$ in both situations. That the Zhang-Rice singlet has a much greater energy gain is due to the fact that the hybridization between $|\underline{c}d^{10};d^9\underline{L}\rangle$ and $|\underline{c}d^{10};d^{10}\underline{L}^2\rangle$ is $\sqrt{2}$ times as large than the hybridization between $|\underline{c}d^{10}\underline{L};d^9\rangle$ and $|\underline{c}d^{10}\underline{L};d^{10}\underline{L}\rangle$. This effect is so strong that charge separation is still more favorable down to values of Q around 4 eV. The presence of d^8 states with a similar hybridization with the $d^9\underline{L}$ configuration only further stabilizes the Zhang-Rice singlet.

Thus the lowest final state has mainly d^{10} character on the CuO_4 unit with the core hole potential. The hole has moved to a neighboring CuO_4 unit. To get more quantitative information on how much of this character is in the lowest final state, we have calculated its overlap with a state which is a linear combination of a d^{10} configuration on the central CuO_4 unit and a Zhang-Rice singlet on either the left or the right CuO_4 unit:

$$\frac{1}{\sqrt{2}}(\langle\text{ZR;0 holes;1 hole}|+\langle\text{1 hole;0 holes;ZR}|)|\text{lowest }E^F(\text{3 holes})\rangle=0.89\ .$$

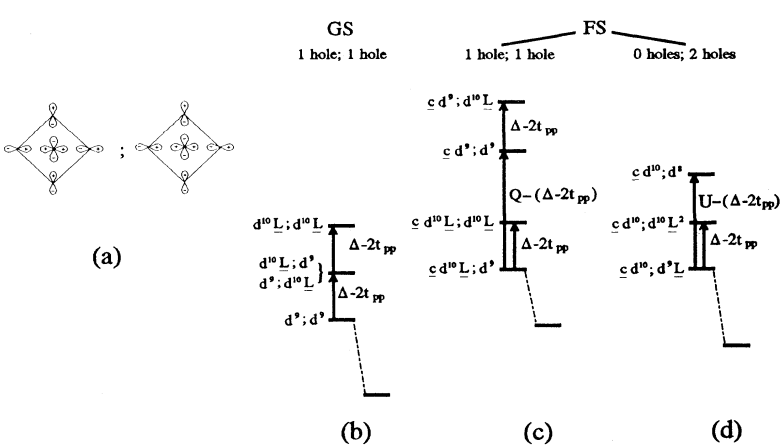

FIG. 5. Energy level diagram for two separate CuO_4 clusters [see (a)]. The levels at the end of the dashed lines show the effect of hybridization on the lowest eigenstate. From left to right: (b) one hole on each CuO_4 cluster. After removal of a core electron there are two possibilities: (c) one hole on each CuO_4 cluster, with a core hole on one of these clusters, (d) both holes on the CuO_4 cluster without the core hole.

This means that the lowest final state has 79% of this character.

It should be stressed that the charge transfer, leading to a d^{10} configuration for the site with the Cu 2p hole and approximate Zhang-Rice singlets on the neighboring site, is a result of the strong core-hole potential. It is therefore a final-state effect and not an indication of mixed valence states in the ground state.[18]

We can therefore conclude that the interpretation of the Cu 2p spectrum should be altered. The satellite is still of mainly $3d^9$ character, but the main peak is split into two components. One peak at higher binding energies corresponds approximately to the original interpretation of the main line with mainly $3d^{10}\underline{L}$ character. In addition a large peak appears, which corresponds to a situation where the hole moves away from the site that it previously occupied, due to the strong core-hole repulsion and forms a Zhang-Rice singlet on a neighboring CuO_4 unit. The copper site with the Cu 2p hole has now a configuration, which is close to d^{10}.

V. DOPING DEPENDENCE OF THE Cu 2p SPECTRUM

For high-T_c compounds, hole doping plays an important role. Since the Cu 2p spectra are usually rather sensitive to the hole doping it is interesting to find out what the underlying mechanism for these changes is. So far it has been assumed that the doped compound can be divided into a system with divalent and trivalent Cu atoms.[19,20] For the formally divalent atoms one then assumes a similar interpretation as for CuO. For a CuO_4 unit with three holes the main line is expected to be of mainly $3d^{10}\underline{L}^2$ character and the satellite of $3d^9\underline{L}$ hole character.

The use of a Cu_3O_{10} cluster also offers the possibility of studying hole doping of 33%. The result of the calculation is shown in Fig. 6(d). For the assignment of the peaks the hole densities have been calculated. In the ground state [see Fig. 4(c)], there is now an extra hole which forms a Zhang-Rice singlet. The chance of finding a Zhang-Rice singlet on a particular CuO_4 unit is approximately equal for all three CuO_4 units.

The hole densities in the lowest final state after introduction of a core hole on the central Cu site are shown in Fig. 4(d). The changes in the hole density for the lowest final state for the four-hole system look very similar to that of the undoped system. Again we observe a decrease of hole density on the central Cu site and the oxygen orbitals 5 and 6. The largest increase in hole density is not on the oxygen orbitals around the central Cu atom, as would be expected for a state with mainly $3d^{10}\underline{L}^2$ character, but on the neighboring CuO_4 units.

To estimate the amount of $3d^{10}$ character on the central CuO_4 unit the overlap of the lowest final state with a state, that consists of a linear combination of a $3d^{10}$ configuration on the central CuO_4 unit and Zhang-Rice singlets on the CuO_4 units at the edges of the Cu_3O_{10} cluster, is calculated

$$\langle \mathrm{ZR;0\ holes;ZR} | \text{lowest } E^F(4 \text{ holes}) \rangle = 0.87 ,$$

which corresponds to 76% of this character.

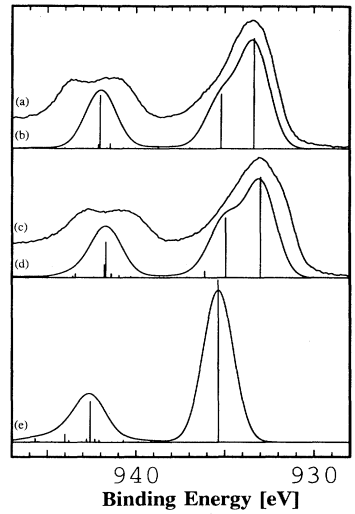

FIG. 6. Comparison of the undoped and 33% doped Cu_3O_{10} cluster with experimental data (see Ref. 31). From top to bottom: (a) Cu $2p^{3/2}$ spectrum of $Bi_2Sr_2YCu_2O_{8.51}$ (0.01 holes per CuO_4 unit), (b) calculated Cu 2p spectrum for the Cu_3O_{10} cluster with three holes, (c) Cu $2p^{3/2}$ spectrum of $Bi_2Sr_2CaCu_2O_{8.23}$ (0.23 holes per CuO_4 unit), (d) calculated Cu 2p spectrum for the Cu_3O_{10} cluster with four holes (0.33 holes per CuO_4 unit), (e) calculated Cu 2p spectrum for a Cu_2O_7 cluster with four holes ($Q=7.7$ in all the calculations).

The conclusion is that the core-hole potential repels the Zhang-Rice singlets from the central CuO_4 unit. This is also confirmed by a calculation where the core-hole potential is put at the left side of the cluster. Here the hole density is largest at the opposite side of the Cu_3O_{10} cluster.

We suggest a peak assignment which is similar to that of the undoped cluster. The lowest eigenstate still has mainly $3d^{10}$ character. The hole(s) have moved to a neighboring CuO_4 unit, thereby forming a Zhang-Rice singlet. The other peaks we propose to be of mainly $3d^{10}\underline{L}$ hole character for the second peak and $3d^9$ character for the satellite.

The spectra have also been compared with experimental data. Cu 2p spectra of $Bi_2Sr_2YCu_2O_{8.51}$ and $Bi_2Sr_2CaCu_2O_{8.23}$ with a hole density of 0.01 and 0.23, respectively, are shown in Figs. 6(a) and 6(c) (for more experimental details see Ref. 31). Some discrepancies are observed. First, the satellite region does not have the multiplet structure. The neglect of multiplet effects in the calculation will only have minimal effect on the phenomena that were described above. Second, especially in the hole-doped situation the higher binding energy peak of the main line has too much spectral weight. This is due to the limited size of the cluster. To the oxygen orbitals 5 and 6, no Cu sites are attached. This limits the charge-transfer screening between different CuO_4 units, leading to an overestimation of the screening from the oxygen orbitals nearest to the Cu site with the core hole. Therefore calculations on larger cluster sizes are necessary to obtain a more reasonable ratio between the two peaks of the main line.

The revised explanation shows that the width of the main peak is not simply due to oxygen-banding effects of the $3d^{10}\underline{L}$ peak. Furthermore it gives a broadening when hole doping the cluster as is also observed in experiment. For the hole-doped system, an increase of the local screening (second peak) with respect to the intersite screening is observed. This can be physically understood from the presence of Zhang-Rice singlets in the system. For intersite screening an electron should come from a neighboring CuO_4 unit. However, introducing an extra hole on a CuO_4 unit with a Zhang-Rice singlet would lead to a state which is at high energy, so this process is much less probable. This leads to a relative decrease of the first peak with respect to the second. The intensity between the satellite and the main peak however hardly changes (0.40 for the undoped and 0.39 for the doped system). This is also observed for the $Bi_2Sr_2Ca_{1-x}Y_xCu_2O_{8+\delta}$ series, where the intensity ratio is 0.37 ± 0.02 over the hole series, $x=0.0-1.0$.

A 100% doped system is shown in Fig. 6(c). To limit the size of the problem the calculation has been done for a Cu_2O_7 cluster. This situation is comparable to formally trivalent $NaCuO_2$. The most important effect is the narrowing of the main line. A study of the hole densities reveals that this state has mainly $3d^{10}\underline{L}^2$ character, as was already suggested by other groups.[20,32] The disappearance of the nonlocal contribution can be understood as follows. For this effect to be energetically more favorable it is necessary to create Zhang-Rice singlets on neighboring CuO_4 units. For the 100% doped system this is no longer possible, since every CuO_4 unit is already occupied by a Zhang-Rice singlet. Therefore the screening is local, which explains the narrow main line. This is also observed in the hole densities. The introduction of a core hole hardly influences the hole density on the neighboring CuO_4 unit.

Similar effects are already observed for the 50% doped system of Fig. 2(b) (the second peak is attributed to oxygen band effects). The lowest final state has here mainly $3d^{10}\underline{L}$ character with the Zhang-Rice singlet on the other CuO_4 unit.

VI. CONCLUSION

In summary we have found that the original interpretation of the Cu $2p$ spectrum is inadequate. A peak appears at the lower binding energy of the $3d^{10}\underline{L}$ peak, which is a result of a charge-transfer screening between neighboring CuO_4 units. The peak assignment for the hole-doped system is very similar. A Zhang-Rice singlet, which might originally have been on the CuO_4 unit where the core hole is created, moves to a neighboring CuO_4 unit due to the presence of the strong Coulomb repulsion of the core hole. For the 100% doped system, cf. $NaCuO_2$, the creation of Zhang-Rice singlets on neighboring CuO_4 units is not possible and the screening is local, leading to a narrow main line.

The calculations also clearly explain the broad and asymmetric shape of the main peak. These intersite charge-transfer screening effects are also possible in other transition metal compounds. However this mechanism is more important for CuO and the high-T_c compounds due to the large stabilization energy of the two hole $^1A_1$ states. However, it offers a possible explanation for the well-known double-peaked structure of the main line in NiO. The extra peak now appears at the high-binding energy side of the usual $3d^9\underline{L}$ peak.[33]

ACKNOWLEDGMENTS

This work was supported by the Nederlandse Stichting voor Fundamenteel Onderzoek der Materie (FOM), the Stichting Scheikundig Onderzoek in Nederland (SON) both financially supported by the Nederlandse Organisatie voor Wetenschappelijk Onderzoek (NWO).

[1]K. S. Kim, J. Electron Spectrosc. Relat. Phenom. **3**, 217 (1974).
[2]A. Rosencwaig, G. K. Wertheim, and H. J. Guggenheim, Phys. Rev. Lett. **27**, 479 (1971).
[3]A. Kotani and Y. Toyozawa, J. Phys. Soc. Jpn. **35**, 1073 (1973); **37**, 912 (1974).
[4]S. Larsson, Chem. Phys. Lett. **40**, 362 (1976); S. Larsson and M. Braga, *ibid.* **48**, 596 (1977).
[5]G. van der Laan, C. Westra, C. Haas, and G. A. Sawatzky, Phys. Rev. B **23**, 4369 (1981).
[6]O. Gunnarsson and K. Schönhammer, Phys. Rev. B **23**, 4315 (1983).
[7]J. Zaanen, C. Westra, and G. A. Sawatzky, Phys. Rev. B **33**, 8060 (1986).
[8]A. E. Bocquet, T. Mizokawa, T. Saitoh, H. Namatame, and A. Fujimori (unpublished).
[9]A. E. Bocquet, T. Saitoh, T. Mizokawa, and A. Fujimori, Solid State Commun. **83**, 11 (1992).
[10]J. Park, S. Ryu, M. Han, and S.-J. Oh, Phys. Rev. B **37**, 10 867 (1988).
[11]A. Kotani, H. Mizuto, T. Jo, and J. C. Perlebas, Solid State Commun. **53**, 805 (1985).
[12]J. C. Fuggle, O. Gunnarsson, G. A. Sawatzky, and K. Schönhammer, Phys. Rev. B **37**, 1103 (1988).
[13]H. Ogasawara, A. Kotani, R. Potze, G. A. Sawatzky, and B. T. Thole, Phys. Rev. B **44**, 5465 (1991).
[14]A. Fujimori, E. Takayama-Muromachi, Y. Uchida, and B. Okai, Phys. Rev. B **35**, 8814 (1987).
[15]Z. X. Shen, J. W. Allen, J. J. Yeh. J.-S. Kang, W. Ellis, W. Spicer, I. Lindau, M. B. Maple, Y. D. Dalichaouch, M. S. Torikachvili, J. Z. Sun, and T. H. Geballe, Phys. Rev. B **36**, 8414 (1987).
[16]D. D. Sarma and A. Taraphder, Phys. Rev. B **39**, 11 570 (1989).
[17]K. Karlsson, O. Gunnarsson, and O. Jepsen, J. Phys. C **4**, 2801 (1992).
[18]F. Parmigiani and G. Samoggia, Europhys. Lett. **7**, 543 (1988).
[19]M. De Santis, A. Bianconi, A. Clozza, P. Castrucci, A. Di Cicco, M. De Simone, A. M. Flank, P. Lagarde, J. Budnick, P. Delogu, A. Gargano, R. Giorgi, and T. D. Makris, in *Proceedings of the International Symposium on the Electronic Structure of High-T_c Superconductors, Rome 1988,* edited by A. Bianconi and A. Marcelli (Pergamon, Oxford, 1989).

[20]P. Steiner, V. Kinsinger, I. Sander, B. Siegwart, S. Hüfner, C. Politis, R. Hoppe, and H. P. Müller, Z. Phys. B **67**, 497 (1987).
[21]H. Eskes, L. F. Feiner, and G. A. Sawatzky, Physica C **160**, 424 (1989).
[22]H. Eskes, L. H. Tjeng, and G. A. Sawatzky, Phys. Rev. B **41**, 288 (1990).
[23]H. Eskes and G. A. Sawatzky, Phys. Rev. B **43**, 119 (1991).
[24]M. S. Hybertsen, E. B. Stechel, W. M. C. Foulkes, and M. Schlüter, Phys. Rev. B **45**, 10 032 (1992).
[25]H. Eskes and G. A. Sawatzky, Phys. Rev. Lett. **61**, 1415 (1988).
[26]J. C. Slater and G. F. Koster, Phys. Rev. **94**, 1498 (1954).
[27]K. Okada and A. Kotani, J. Phys. Soc. Jpn. **58**, 2578 (1989).
[28]A. K. McMahan, R. M. Martin, and S. Satpathy, Phys. Rev. B **38**, 6650 (1988).
[29]M. S. Hybertsen, M. Schlüter, and N. E. Christensen, Phys. Rev. B **39**, 9028 (1989).
[30]F. C. Zhang and T. M. Rice, Phys. Rev. B **37**, 3759 (1988).
[31]M. A. van Veenendaal, R. Schlatmann, W. A. Groen, and G. A. Sawatzky, Phys. Rev. B **47**, 446 (1993).
[32]T. Mizokawa, H. Namatame, A. Fujimori, H. Kondoh, H. Kuroda, and N. Kosugi, Phys. Rev. Lett. **67**, 1638 (1991).
[33]M. A. van Veenendaal and G. A. Sawatzky (unpublished).